CrystEngComm

PAPER

View Article Online
View Journal | View Issue

Cite this: *CrystEngComm*, 2015, **17**, 540

# Self-assembly of alumina nanowires into controllable micro-patterns by laser-assisted solvent spreading: towards superwetting surfaces†

Meiling Lv,[a] Qianbin Wang,[a] Qing'an Meng,[a] Tianyi Zhao,*[a] Huan Liu*[a] and Lei Jiang[ab]

Received 10th July 2014,
Accepted 21st August 2014

DOI: 10.1039/c4ce01434k

www.rsc.org/crystengcomm



Self-assembly of nanowires into micro-scale patterns, especially in a controlled manner, has received increasing research interest because of the wide variety of potential applications, including micro-optics and electronic devices, as well as nanomaterials-based energy conversion systems. In this contribution, a novel laser-assisted solution spreading method was developed to fabricate and self-assemble alumina nanowires (ANWs) into large-scale 3-dimensional (3D) micro-patterned surfaces in one step. Here, sodium hydroxide (NaOH) solution played a dual role, both chemically etching the anodic aluminum oxide template (AAO) into ANWs and self-assembling the as-obtained ANWs into micro-patterns under capillary force. It is notable that the micro-scale patterns can be artificially controlled by introducing laser points before solution spreading on the AAO template, and thus the laser-etched area will act as the fixation point during the ANW assembly process. Moreover, the as-prepared micro-patterned ANW film exhibits typical micro-/nano-hierarchical surface topology and shows superhydrophilicity. The film can be transformed into a superhydrophobic surface by chemical modification with 1*H*,1*H*,2*H*,2*H*-perfluorodecyltriethoxysilane (FAS). Here, by taking advantage of wetting and dewetting processes of a solution on an AAO template, we propose a facile method that enables the fabrication of 3D micro-patterned ANW surfaces, which have superwetting properties. We envisage that this method could shed new light on the fabrication of functional micro-patterned devices where a one-dimensional nano-material and solution phase are involved.

## Introduction

Self-assembly is a fundamental principle and regularly used technique which provides autonomous organization of pre-existing components into well-ordered patterns or structures.[1–6] Molecular self-assembly is the most well-studied subfield, which enables the fabrication of novel supermolecular architectures *via* weak, noncovalent interactions such as hydrogen bonds, electrostatic interactions, hydrophobic interactions, and van der Waals interactions.[7–15] However, utilizing a long range force (such as capillary force, surface tension or convection) to construct well-patterned structures *via* a self-assembly approach at the nano-/mesoscale level has been little reported, and appears to be important in diverse applications in chemical/biomolecular sensing,[16,17] nanoscale electronic circuits,[18,19] optoelectronics,[20–22] and novel energy conversion systems.[23,24] Recently, it has been proposed that the capillary force is applicable to the self-assembly of micrometer or even millimeter scale components into patterned structures.[25–28] For example, Aizenberg and coworkers reported an assembly strategy based on capillary force-induced aggregation of mesoscale pillars made by soft lithography.[4] Recently, by utilizing a water spreading method, we have realized the self-assembly of an aligned carbon nanotube array into 3-dimensional (3D) micrometer-scale patterns driven by the capillary force generated during the dewetting process.[25,29] So far, the capillary force has been utilized to self-assemble various nano-materials such as carbon nanotubes, polymer nanopillars and inorganic nanowires into micro-patterned structures, and some new functions were generated as a result.[30–36] However, all these techniques suffer from the limitation of needing to prepare nanometer-scale components before the assembly, where complicated chemical and physical processes are often required. On the other hand, self-assembly of nano-materials, especially one-dimensional (1D) nanomaterials, in a controllable manner remains a challenge, mainly because of the difficulty of

[a] *Key Laboratory of Bio-Inspired Smart Interfacial Science and Technology of Ministry of Education, Beijing Key Laboratory of Bio-inspired Energy Materials and Devices, School of Chemistry and Environment, BeiHang University, Beijing, 100191, PR China. E-mail: liuh@buaa.edu.cn, zhaoty@buaa.edu.cn*

[b] *Beijing National Laboratory for Molecular Sciences, Key Laboratory of Organic Solids, Institute of Chemistry, Chinese Academy of Sciences, Beijing 100190, PR China*

† Electronic supplementary information (ESI) available. See DOI: 10.1039/c4ce01434k

spatially controlling the assembly center.[37–39] To date, strategies that can generate tunable 3D architectures from 1D nanostructures in a controllable manner in one step remain a challenge and are poorly understood.

Herein, we developed a facile approach using a laser-assisted solution spreading method, which enables one-step fabrication and self-assembly of 1D alumina nanowires (ANWs) into 3D micro-patterns in a controlled manner starting from the anodic aluminum oxide template (AAO), with a synergistic effect of chemical etching and capillary-induced bending of the ANWs. The as-generated micro-patterned surfaces exhibited typical micro/nano-hierarchical topologies, where unique superwetting phenomena were observed. This technique allows the fabrication and patterning of nanowires in one step, and consequently enables a dual-scale structured surface with typical wettability.

## Experimental

### 2.1. Materials and equipment

AAO with a diameter of 200 nm was purchased from Wako Chemicals Inc. The 1*H*,1*H*,2*H*,2*H*-perfluorodecyltriethoxysilane (FAS) was purchased from Sigma-Aldrich. Ethanol ($CH_3CH_2OH$) and sodium hydroxide (NaOH) were purchased from Beijing Chemical Works and were used without any further purification.

### 2.2. Preparation of 3D ANWs

The AAO was successively washed with ethanol and deionized water several times and then dried under a nitrogen atmosphere. 2 μL aqueous NaOH solution with a concentration of 2 mol $L^{-1}$ was dripped onto the surface of the AAO so that the NaOH solution would naturally permeate into the AAO. Then, the treated AAO was rinsed with purified water ten times and dried under a nitrogen atmosphere.

### 2.3. Morphology control of the micro-structure

The surface morphology of the as-prepared 3D micro-patterns was controlled by setting the chemical etching time to 1, 3, 4, 5, 7 and 8 min respectively. Here, 5 min was the most suitable time to enable the fabrication and self-assembly of ANWs in a controllable manner. A pulse laser etching system with a wavelength of 355 nm (New Wave Research Inc., California) was used to control the morphology of the AAOs before the chemical etching process, where the laser etching points were artificially designed, and the size of the facula was 35 × 35 (2–3 μmm) with an energy of 1.8–2.9 mW. The morphology observation of the as-prepared 3D ANWs was conducted using a scanning electron microscope (SEM, Hitachi S-4800, Japan).

### 2.4. Chemical modification of various surfaces with fluorosilane and wettability characterization

The chemical modification of both the micro-patterned surfaces and the AAOs was performed by immersing the substrates in a 1% (volume ratio) ethanol solution of 1*H*,1*H*,2*H*,2*H*-perfluorodecyltriethoxysilane (FAS) for 48 h at room temperature, after which they were removed and treated in an oven at 120 °C for 1 h.

The surface wettability was characterized by measuring the water contact angles using a OCA20 contact angle system (Data-Physics, Germany). Water droplets of 3 μL were used as the probe liquid for the CA measurements, and the values reported were the average of at least five drops per sample at different locations.

## Results and discussion

The strategy of the laser-assisted solution spreading method is schematically illustrated in Fig. 1. As Fig. 1a indicates, we first spread the NaOH solution directly onto an AAO substrate to check the feasibility of the method. The NaOH solution spread and penetrated into the AAO substrate rapidly once dropped onto the AAO (Fig. 1a), and subsequently many nanowire structures (Fig. S1†) could be observed on the surface of the AAO due to the chemical etching effect.[40] Here, the alumina chemical nature of the as-prepared nanowires was confirmed by X-ray photoelectron spectroscopy (Fig. S1†). It is suggested that the chemical etching could proceed in a controllable manner by setting a suitable etching time in order to generate nanowires with optimized length, and the

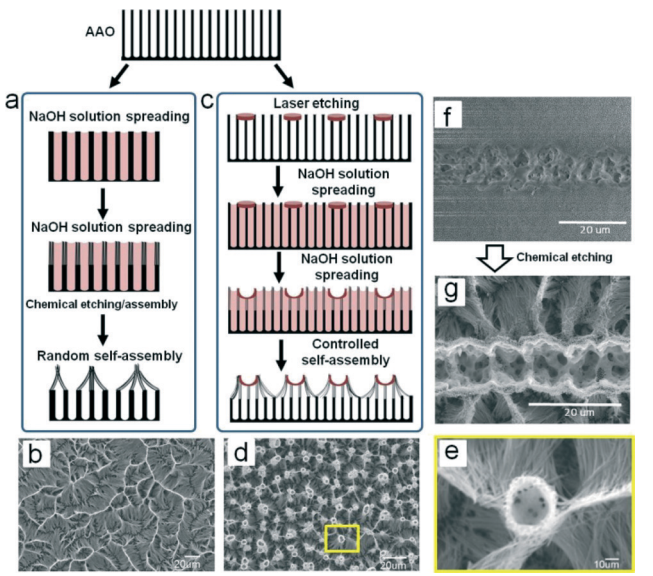


Fig. 1 Schematic illustration of the laser-assisted solution spreading method and representative SEM images of the as-prepared micro-patterned ANWs. (a) Directly spreading NaOH solution onto the AAO substrate and (b) the resulting irregular micro-patterned ANWs. (c) Spreading NaOH solution onto an AAO substrate pre-treated by a pulse laser and (d) the resulting regular micro-patterned ANWs. (e) The high-magnification image of one laser point after performing the solution spreading procedure, where the laser point acts as the assembly center of the ANWs. (f) and (g) show the typical SEM images of the AAO substrate after pre-treating by pulse laser and then after solution spreading, respectively.

details of this will be mentioned later. After a certain period of chemical corrosion, the AAO was taken out of the NaOH solution to terminate the chemical etching and was subsequently washed with water. During the whole process, the liquid phase was trapped in the intervals between the nanowires and replaced by a vacuum from bottom to top, resulting in a concave structure of the nanowires because of the constant capillary force from bottom to top. Consequently, the ANWs were bended into bundles in a random manner as a result of self-assembly (Fig. 1a), driven by capillary force-induced water dilation stress.[25,29] Due to the uncontrollability of the capillary force direction, such a self-assembly process will result in irregular 3D patterns (Fig. 1a and b). The SEM image of the as-prepared surface (Fig. 1b) clearly shows the formation of the patterned ANW bundles on a large scale. This demonstrates that such a solution spreading method can enable the fabrication and self-assembly of ANWs in one step.

In order to control the self-assembly process – specifically, in order to control the position where the ANWs bundles formed – a pulse laser was used to introduce defects on the AAO substrate before the NaOH solution spreading. As shown schematically in Fig. 1c, the pulse laser was applied to etch the AAO substrate in a controllable manner, in order to introduce patterned defects on the surface of the AAO substrates. In the laser-assisted procedure, because of the high energy involved, the laser can provide a significant amount of heat with a temperature higher than the melting point of alumina, such that the pulse laser destroys the irradiated area of the template surface, forming a solid point structure instead of the original porous structure after congealing at room temperature (laser-etched AAO surfaces are shown in Fig. 1f). After laser etching, the spreading of NaOH solution on the pre-treated AAO was carried out to generate and then self-assemble nanowires (Fig. 1c). As a result of the laser irradiation, the destroyed areas (defect points) underwent a much slower chemical etching process by the NaOH solution compared to the non-destroyed parts. Therefore, the intact porous structure of the non-destroyed areas is chemical etched into ANWs (Fig. 1c and g), but the laser-etched melted parts (the defect points) remain almost the same with standing structures. Similarly, during the solution evaporation process, the capillary force drives the nanowires to assemble into bundles. However, the laser-etched points are relatively large and will not be reduced in size by the capillary effect-induced tensile force.[4,25] As a result, the nanowires tend to flatten towards laser-etched sites, which act as centres for ANWs to self-assemble into bundles (Fig. 1d). The typical SEM image of the AAOs treated by the laser-assisted method is presented in Fig. 1e. It can be observed that all the nanowires assembled into bundles with the laser-etched points as centres (Fig. 1e). Taken together, we can conclude that controllable ordered 3D micro-/nanocomposite patterns of ANWs can be obtained by a laser-assisted solution spreading method in one step, whereas non-laser-assisted solution spreading results in random ANWs bundles.

It has therefore been demonstrated that micro-patterned ANWs could be programmably fabricated by a laser-assisted solution spreading method. As presented in Fig. 2a and b, when AAOs were pre-etched by a pulse laser with a lattice structure and then chemically etched with an NaOH solution for about 5 min, it can be clearly observed that ANWs near the laser lines self-assemble into regular bundles with the laser points as centres (region 1 in Fig. 2b), while for the other regions, ANWs freely self-assemble into irregular patterns with no obvious centre (region 2 in Fig. 2b) since they are too far away from the laser line. These results clearly indicate that laser etching is the crucial factor for generating regular assembly of ANWs. Moreover, we found that decreasing the distances between laser lines to a suitable extent could allow well-controlled ANW patterns with laser-etched points as centres. As shown in Fig. 2, with a decreasing distance between laser lines from *ca.* 62 μm (Fig. 2a) to 30 μm (Fig. 2c) and 19 μm (Fig. 2d), the freely assembling region deceased and the regularly assembling region increased in size accordingly. In particular, when the distance decreased to *ca.* 19 μm (Fig. 2d), the freely assembling region disappeared completely and all nanowires assembled into bundles with laser points as centres. Further detailed experiments demonstrated that if the average distances between laser lines were controlled in the range of 18–25 μm, all ANWs would regularly assemble with the nearest laser point as the centre. The mechanism of the ordered assembly can be attributed to the capillary force, which is the critical factor that causes the nanowires to collapse into bundles as illustrated in Fig. 1. However, during the collapsing process, the anisotropic capillary force could only act on the region near the laser etching points, as presented in Fig. 2b. According to

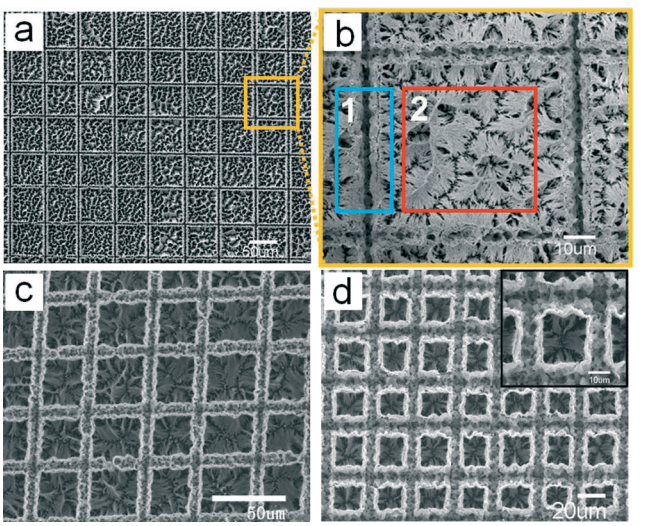


Fig. 2 Representative SEM images of the as-prepared micro-patterned ANWs fabricated by the laser-assisted solution spreading method. The patterns were obtained with decreasing average distances between the two adjacent laser lines of *ca.* 62 μm (a), 30 μm (c) and 19 μm (d). (b) The magnified image of (a) showing the typical two regions of ANW bundles: the randomly bended region (framed in red) and the regularly bended region (framed in blue).

the experimental results, a distance between the laser points in the range of 18–25 μm is beneficial in order for the nanowires to self-assemble into regular bundles. We can therefore conclude that the size and composition of 3D microscale patterns can be programmably controlled by tuning the distribution of the laser etched area.

By designing the laser etching pattern, we can obtain various micro-patterned ANWs in a straightforward manner using the solution spreading method, as shown in Fig. 3. In our experiment, we adjusted the frequency and motion speed of the laser points to ensure that each laser point could be separated from the others. In the procedure, we first pre-patterned the AAO surface with lattice (Fig. 3a), parallel line (Fig. 3b), double point (Fig. 3c) or double line (Fig. 3d) structures by laser etching, and then let the NaOH solution spread onto these pre-patterned AAO substrates for 5 min. It can be observed that all nanowires lodged towards the laser points and formed a microscale volcano-like structure. Especially when the surface was laser-etched with double points (Fig. 3c) and double lines (Fig. 3d), the nanowires lodged toward the nearest laser points. Therefore, we can design any pattern by controlling the laser etching distribution and can obtain micro-/nanocomposite structures without preparing the nanowires in advance.

Here, the chemical etching time was noted as a crucial factor for building ANWs. The SEM images of ANWs prepared with different etching times are shown in Fig. 4. It can be concluded that the length of nanowire increased with extended etching time as presented in Fig. 4a to e. During the initial stage of etching (less than 4 min), AAO can be gradually etched into short nanowires standing separately from each other which do not show bending tendencies (Fig. 4a–c), due to the rigidity of the nanowires.[13,29] However, if we increased the etching time to 5–7 min, the nanowires were elongated and could be up to 50–200 nm (Fig. 4d and e). We found that the nanowires began to bend and deform

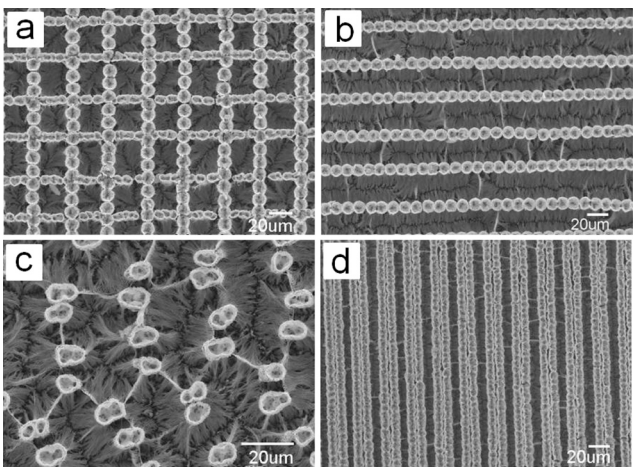


Fig. 3 Several representative micro-patterned ANWs prepared by the laser-assisted solution spreading method on AAOs that were pre-patterned by laser etching with (a) lattice, (b) parallel line, (c) double point and (d) double line structures.

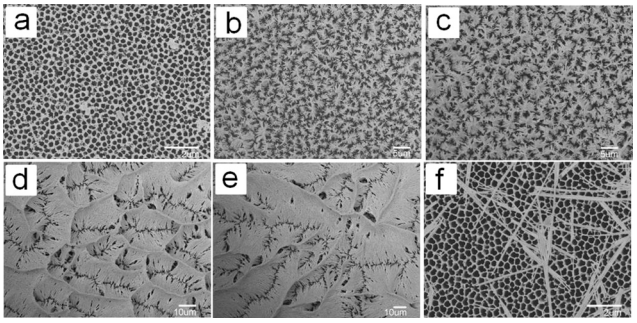


Fig. 4 Time dependence of AAOs etched using 2 mol $L^{-1}$ NaOH solvent with etching times of (a) 1 min, (b) 3 min, (c) 4 min, (d) 5 min, (e) 7 min and (f) 8.5 min.

into microscale bundle structures at this stage, mainly because the enlarged length-diameter ratio of the ANWs make them more mechanical flexible. With the prolongation of the etching time to 8 min, the nanowires were too long to be broken away from the surface of the AAO (Fig. 4f). Therefore, we considered that 5 min was the most suitable etching time to obtain self-assembled microscale patterns of ANWs, and thus we set the solution spreading time to 5 min in our experiment, as mentioned above. In addition, we found that ANWs could self-assemble into irregular patterns on the non-treated AAO substrates (Fig. 4e), which also highlights the significant role of the laser.

The as-prepared micro-patterned ANW surfaces exhibited a typical micro-/nano-hierarchical topological nature, where the laser points contribute to the microscale patterns and the ANWs from chemical etching by NaOH solution are the nanoscale components. Micro-/nano-hierarchical topology is a widely shared property of many biological surfaces, such as lotus leaf, the leg of a water strider and animal hairs, which normally enables unique surface wettability.[41–44] Here, the micro-patterned ANWs show superwetting behaviour. We estimated the water contact angle (CA) of these surfaces by comparison with that of the original intact AAO. The results indicated that the CA of the micro-patterned ANWs is nearly 0° (Fig. 5a), exhibiting superhydrophilicity where water droplets spread immediately upon contact with the surface, while the original intact AAO substrate had a water CA of 20.9° (Fig. 5b). Moreover, after modification with FAS, the CA of the micro-patterned ANWs changed dramatically to 164.4° (Fig. 5a), showing a typical superhydrophobicity where the water droplet can maintain its spherical shape steadily. By comparison, the original intact AAO substrate gave a water CA of only 132° after chemical modification with FAS (Fig. 5b). The results suggested that the micro-patterned ANW surface can exhibit superwetting behaviour where both superhydrophilicity and superhydrophobicity can be observed.

Schematic illustrations of wetting on the micro-patterned ANWs are proposed in Fig. 5a. The 3D micro-/nanocomposite structure enables a Cassie state contact with a water droplet, where large amounts of air can be trapped at the interface of

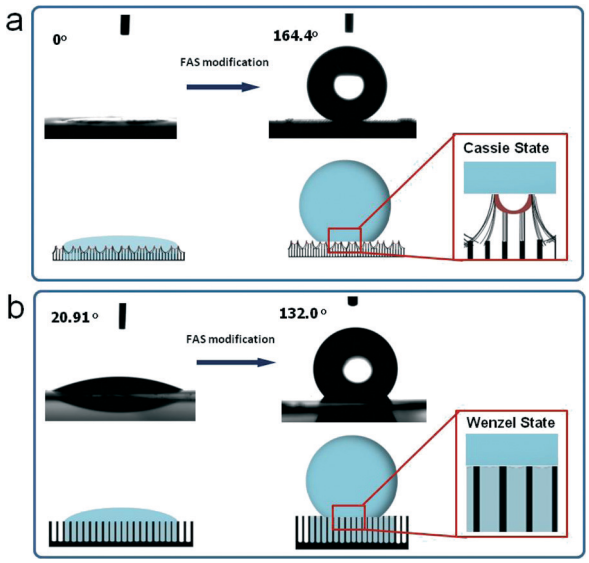


**Fig. 5** (a) Superwetting properties of the micro-patterned ANWs and schematic illustrations indicating the inherent superhydrophilicity and the superhydrophobicity after surface modification with FAS. (b) Wettability properties of the original intact AAO suggested its normal hydrophilicity and hydrophobicity after surface modification with FAS.

water and a rough surface after surface modification of a low surface energy material with FAS.[45–48] Thus, a typical solid–air–water composite interface was formed on contact with a water droplet, giving a high water CA. Meanwhile, the typical surface roughness of micro-patterned ANWs is also favourable for the spreading of water under the assistance of the capillary effect, since the naked ANWs are inherently a high surface energy material.[49] However, for the original intact AAO only nanometer-scale structure was observed, and so the contact between water and the substrate should be in a Wenzel state (Fig. 1b), exhibiting weakened hydrophilicity and hydrophobicity before and after the FAS surface modification, respectively. Such superwetting performance on the micro-patterned ANW surface might lead to new functions.

## Conclusions

In summary, we developed a novel laser-assisted solution spreading method, which enables the fabrication and self-assembly of ANWs into large-scale 3D micro-patterned surfaces in one step. The laser-etched points on the AAO surface acted as the fixation points to guide the self-assembly of the ANWs, while the NaOH solution has two functions, one being the chemical etching of the AAO substrate into ANWs and the other being the generation of the capillary effect that bends the ANWs into bundles. Moreover, the as-prepared micro-patterned ANW film exhibits superwetting properties, with inherent superhydrophilicity that can be turned into superhydrophobicity by chemical modification with FAS. We envisage that this method could shed new light on the fabrication of functional micro-patterned devices where a one-dimensional nano-material and solution phase are involved.

## Acknowledgements

The authors thank the financial support of the National Research Fund for Fundamental Key Projects (2013CB933000), Program for New Century Excellent Talents in University (NCET-13-0024), Fok Ying Tong Education Foundation (132008), National Natural Science Foundation of China (21101010), and the Fundamental Research Fund for the Central Universities.

## Notes and references

1 T. L. Breen, J. Tien, S. R. J. Oliver, T. Hadzic and G. M. Whitesides, *Science*, 1999, **284**, 948–951.
2 A. Ciesielski, C.-A. Palma, M. Bonini and P. Samori, *Adv. Mater.*, 2010, **22**, 3506–3520.
3 D. Chandra and S. Yang, *Acc. Chem. Res.*, 2010, **43**, 1080–1091.
4 B. Pokroy, S. H. Kang, L. Mahadevan and J. Aizenberg, *Science*, 2009, **323**, 237–240.
5 C. Zhu, Y. Fang, D. Wen and S. Dong, *J. Mater. Chem.*, 2011, **21**, 16911–16917.
6 H. Shimoda, S. J. Oh, H. Z. Geng, R. J. Walker, X. B. Zhang, L. E. McNeil and O. Zhou, *Adv. Mater.*, 2002, **14**, 899–901.
7 D. Chandler, *Nature*, 2005, **437**, 640–647.
8 L. Wang, Y. Fu, Z. Wang, Y. Wang, C. Sun, Y. Fan and X. Zhang, *Macromol. Chem. Phys.*, 1999, **200**, 1523–1527.
9 X. Yan, S. Li, J. B. Pollock, T. R. Cook, J. Chen, Y. Zhang, X. Ji, Y. Yu, F. Huang and P. J. Stang, *Proc. Natl. Acad. Sci. U. S. A.*, 2013, **110**, 15585–15590.
10 R. Deng, S. Liu, J. Li, Y. Liao, J. Tao and J. Zhu, *Adv. Mater.*, 2012, **24**, 1889–1893.
11 C.-C. Chu, G. Raffy, D. Ray, A. Del Guerzo, B. Kauffmann, G. Wantz, L. Hirsch and D. M. Bassani, *J. Am. Chem. Soc.*, 2010, **132**, 12717–12723.
12 J. Romulus and M. Weck, *Macromol. Rapid Commun.*, 2013, **34**, 1518–1523.
13 K. K. S. Lau, J. Bico, K. B. K. Teo, M. Chhowalla, G. A. J. Amaratunga, W. I. Milne, G. H. McKinley and K. K. Gleason, *Nano Lett.*, 2003, **3**, 1701–1705.
14 K. Tahara, S. Lei, J. Adisoejoso, S. De Feyter and Y. Tobe, *Chem. Commun.*, 2010, **46**, 8507–8525.
15 K. S. Mali, K. Lava, K. Binnemans and S. De Feyter, *Chem. – Eur. J.*, 2010, **16**, 14447–14458.
16 J.-H. Kim, D. A. Heller, H. Jin, P. W. Barone, C. Song, J. Zhang, L. J. Trudel, G. N. Wogan, S. R. Tannenbaum and M. S. Strano, *Nat. Chem.*, 2009, **1**, 473–481.
17 A. Tao, F. Kim, C. Hess, J. Goldberger, R. R. He, Y. G. Sun, Y. N. Xia and P. D. Yang, *Nano Lett.*, 2003, **3**, 1229–1233.
18 S. A. Dayeh, D. P. R. Aplin, X. Zhou, P. K. L. Yu, E. T. Yu and D. Wang, *Small*, 2007, **3**, 326–332.
19 H. Yan, H. S. Choe, S. Nam, Y. Hu, S. Das, J. F. Klemic, J. C. Ellenbogen and C. M. Lieber, *Nature*, 2011, **470**, 240–244.
20 R. Yan, D. Gargas and P. Yang, *Nat. Photonics*, 2009, **3**, 569–576.

 

21 B. Su, Y. Wu and L. Jiang, *Chem. Soc. Rev.*, 2012, **41**, 7832–7856.
22 Y. Chen, X. Ding, S.-C. S. Lin, S. Yang, P.-H. Huang, N. Nama, Y. Zhao, A. A. Nawaz, F. Guo, W. Wang, Y. Gu, T. E. Mallouk and T. J. Huang, *ACS Nano*, 2013, **7**, 3306–3314.
23 Q. Yang, Y. Liu, C. Pan, J. Chen, X. Wen and Z. L. Wang, *Nano Lett.*, 2013, **13**, 607–613.
24 R. Yu, C. Pan and Z. L. Wang, *Energy Environ. Sci.*, 2013, **6**, 494–499.
25 H. Liu, S. H. Li, J. Zhai, H. J. Li, Q. S. Zheng, L. Jiang and D. B. Zhu, *Angew. Chem., Int. Ed.*, 2004, **43**, 1146–1149.
26 J. G. Fan, D. Dyer, G. Zhang and Y. P. Zhao, *Nano Lett.*, 2004, **4**, 2133–2138.
27 M. A. Correa-Duarte, N. Wagner, J. Rojas-Chapana, C. Morsczeck, M. Thie and M. Giersig, *Nano Lett.*, 2004, **4**, 2233–2236.
28 H. Duan and K. K. Berggren, *Nano Lett.*, 2010, **10**, 3710–3716.
29 H. Liu, J. Zhai and L. Jiang, *Soft Matter*, 2006, **2**, 811–821.
30 N. Bowden, S. R. J. Oliver and G. M. Whitesides, *J. Phys. Chem. B*, 2000, **104**, 2714–2724.
31 D. B. Wolfe, A. Snead, C. Mao, N. B. Bowden and G. M. Whitesides, *Langmuir*, 2003, **19**, 2206–2214.
32 M. Sano, A. Kamino, J. Okamura and S. Shinkai, *Nano Lett.*, 2002, **2**, 531–533.
33 J. Jin, T. Iyoda, C. S. Cao, Y. L. Song, L. Jiang, T. J. Li and D. Ben Zhu, *Angew. Chem., Int. Ed.*, 2001, **40**, 2135–2138.
34 W. T. S. Huck, J. Tien and G. M. Whitesides, *J. Am. Chem. Soc.*, 1998, **120**, 8267–8268.
35 E. Palleau, N. M. Sangeetha, G. Viau, J.-D. Marty and L. Ressier, *ACS Nano*, 2011, **5**, 4228–4235.
36 J. Yu, C. Geng, L. Zheng, Z. Ma, T. Tan, X. Wang, Q. Yan and D. Shen, *Langmuir*, 2012, **28**, 12681–12689.
37 X. Zhang, X. Zhang, K. Zou, C.-S. Lee and S.-T. Lee, *J. Am. Chem. Soc.*, 2007, **129**, 3527–3532.
38 Q. X. Tang, H. X. Li, M. He, W. P. Hu, C. M. Liu, K. Q. Chen, C. Wang, Y. Q. Liu and D. B. Zhu, *Adv. Mater.*, 2006, **18**, 65–68.
39 H. Cui, Y. Sun and C. X. Wang, *CrystEngComm*, 2013, **15**, 5376–5381.
40 G. Meng, T. Yanagida, K. Nagashima, T. Yanagishita, M. Kanai, K. Oka, A. Klamchuen, S. Rahong, M. Horprathum, B. Xu, F. Zhuge, Y. He, H. Masuda and T. Kawai, *RSC Adv.*, 2012, **2**, 10618–10623.
41 K. Liu, X. Yao and L. Jiang, *Chem. Soc. Rev.*, 2010, **39**, 3240–3255.
42 T. Sun, L. Feng, X. Gao and L. Jiang, *Acc. Chem. Res.*, 2005, **38**, 644–652.
43 Y. Li, G. Duan, G. Liu and W. Cai, *Chem. Soc. Rev.*, 2013, **42**, 3614–3627.
44 Y. Li, N. Koshizaki, H. Wang and Y. Shimizu, *ACS Nano*, 2011, **12**, 9403–9412.
45 S. Wang and L. Jiang, *Adv. Mater.*, 2007, **19**, 3423–3424.
46 Q. Wang, M. Safdar, X. Zhan and J. He, *CrystEngComm*, 2013, **15**, 8475–8482.
47 S. Dai, D. Zhang, Q. Shi, X. Han, S. Wang and Z. Du, *CrystEngComm*, 2013, **15**, 5417–5424.
48 H. Cao, Y. Xiao and R. Liang, *CrystEngComm*, 2011, **13**, 5688–5691.
49 D. Gu and F. Schuth, *Chem. Soc. Rev.*, 2014, **43**, 313–344.